

The structure guided discovery of a selective Mcl-1 inhibitor with cellular activity

Zoltan Szlavik, Levente Ondi, Marton Csekei, Attila Paczal, Zoltan B Szabo, Gabor Radics, James B Murray, James Davidson, I-Jen Chen, Ben Davis, Roderick E Hubbard, Christopher Pedder, Pawel Dokurno, Allan E. Surgenor, Julia Smith, Alan Robertson, Gaetane Le Toumelin-Braizat, Nicolas Cauquil, Marion Zarka, Didier Demarles, Francoise Perron-Sierra, Audrey Claperon, Frederic Colland, Olivier Geneste, and András Kotschy

J. Med. Chem., **Just Accepted Manuscript** • Publication Date (Web): 24 Jun 2019

Downloaded from <http://pubs.acs.org> on June 25, 2019

Just Accepted

“Just Accepted” manuscripts have been peer-reviewed and accepted for publication. They are posted online prior to technical editing, formatting for publication and author proofing. The American Chemical Society provides “Just Accepted” as a service to the research community to expedite the dissemination of scientific material as soon as possible after acceptance. “Just Accepted” manuscripts appear in full in PDF format accompanied by an HTML abstract. “Just Accepted” manuscripts have been fully peer reviewed, but should not be considered the official version of record. They are citable by the Digital Object Identifier (DOI®). “Just Accepted” is an optional service offered to authors. Therefore, the “Just Accepted” Web site may not include all articles that will be published in the journal. After a manuscript is technically edited and formatted, it will be removed from the “Just Accepted” Web site and published as an ASAP article. Note that technical editing may introduce minor changes to the manuscript text and/or graphics which could affect content, and all legal disclaimers and ethical guidelines that apply to the journal pertain. ACS cannot be held responsible for errors or consequences arising from the use of information contained in these “Just Accepted” manuscripts.

The structure guided discovery of a selective Mcl-1 inhibitor with cellular activity

Zoltan Szlávik,¹ Levente Ondi,^{1†} Márton Csékei,¹ Attila Paczal,¹ Zoltán B. Szabó,¹ Gábor Radics,^{1†}
James Murray,² James Davidson,² Ijen Chen,² Ben Davis,² Roderick E. Hubbard,² Christopher Pedder,²
Pawel Dokurno,² Allan Surgenor,² Julia Smith,² Alan Robertson,² Gaetane LeToumelin-Braizat,³
Nicolas Cauquil,³ Marion Zarka,³ Didier Demarles,⁴ Françoise Perron-Sierra,¹ Audrey Claperon,³
Frederic Colland,³ Olivier Geneste,³ András Kotschy^{1,*}

¹Servier Research Institute of Medicinal Chemistry, Záhony u. 7., H-1031 Budapest, Hungary,

²Vernalis (R&D) Ltd., Granta Park, Cambridge CB21 6GB, UK

³Institute de Recherche Servier, 125 Chemin de Ronde, 78290 Croissy-sur-Seine, France

⁴Technologie Servier, 27 Rue Eugène Vignat, 45000 Orleans, France

Abstract:

Myeloid cell leukemia 1 (Mcl-1), an antiapoptotic member of the Bcl-2 family of proteins, whose upregulation when observed in human cancers is associated with high tumor grade, poor survival, and resistance to chemotherapy, has emerged as an attractive target for cancer therapy. Here we report the discovery of selective small molecule inhibitors of Mcl-1 that inhibit cellular activity. Fragment screening identified thienopyrimidine amino acids as a promising but non-selective hit that were optimized using NMR and X-ray derived structural information. The introduction of hindered rotation along a biaryl axis has conferred high selectivity to the compounds and cellular activity was brought on scale by offsetting the negative charge of the anchoring carboxylate group. The obtained compounds described here exhibit nanomolar binding affinity and mechanism-based cellular efficacy, caspase induction and growth inhibition. These early research efforts illustrate drug

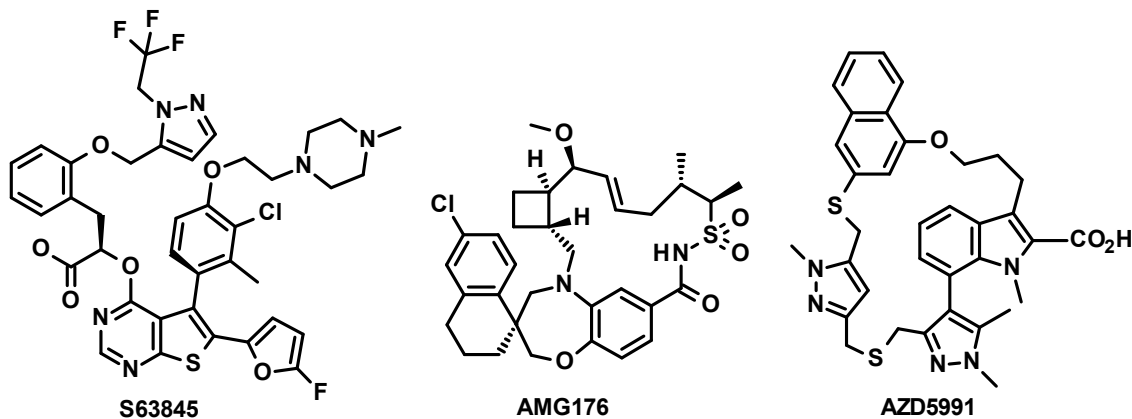
1
2
3 discovery optimisation from thienopyrimidine hits to a lead compound, the chemical series leading
4
5 to the identification of our more advanced compounds S63845 and S64315
6
7
8
9

10 **Introduction**

11 Apoptosis, an evolutionary highly conserved form of programmed cell death, is an essential process
12
13 for the elimination of no longer needed and dangerous cells.¹ Evasion of apoptosis is recognised as a
14
15 critical element of the development as well as sustained expansion of tumours, and also underlies
16
17 resistance to diverse anti-cancer treatments.² Mcl-1 is a member of the Bcl-2 family, critical
18
19 regulatory proteins of the mitochondrial apoptotic pathway, and is frequently upregulated in
20
21 cancer.³ Moreover increased expression of the MCL1 gene through transcriptional or post-
22
23 transcriptional mechanisms was observed as a downstream consequence of several key oncogenic
24
25 pathways.⁴ Mcl-1 is needed to sustain the growth of diverse tumours, including acute myeloid
26
27 leukaemia (AML)⁵, MYC-⁶ or BCR-ABL-driven pre-B/B lymphomas,⁷ certain breast cancers as well as
28
29 Non Small Cell Lung Carcinoma (NSCLC) derived cell lines that carry MCL1 gene amplifications.⁸
30
31 Certain compounds that broadly inhibit gene transcription or protein translation exert their cytotoxic
32
33 effects in tumour cells (at least in part) by downregulating MCL1.⁹
34
35
36
37
38

39 In the clinic, the highly promising activity of the Bcl-2-selective inhibitor venetoclax (Venclexta®),
40
41 which led to its approval in relapsed/refractory Chronic Lymphocytic Leukemia (CLL) patients with
42
43 17p deletion and in AML, has validated the use of drugs that directly activate apoptosis in cancer
44
45 therapy.¹⁰ Until recently only compounds showing weak cellular potency on Mcl-1 (high μ molar
46
47 range) and therefore useful only as in vitro chemical tools were available.¹¹ Starting in late 2016 a
48
49 series of potent and selective Mcl-1 inhibitors were disclosed (Scheme 1) some of which have
50
51 recently also entered clinical development.¹² The long standing interest in Mcl-1 as a target and the
52
53 late emergence of Mcl-1 targeting drug candidates suggests that drugging Mcl-1 is not trivial.
54
55 Supporting this analysis, the present manuscript describes our early research efforts to optimise
56
57
58
59
60

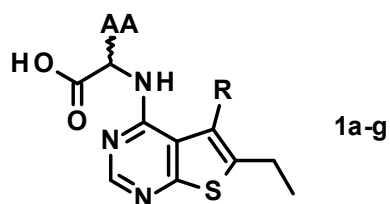
1
2
3 thienopyrimidine hits¹³ to a lead compound on the way to our more advanced compounds S63845
4
5 and S64315 detailing the pitfalls we have encountered in this process.
6
7
8
9

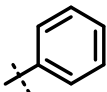
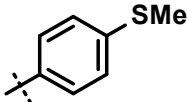
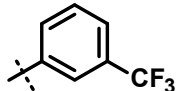
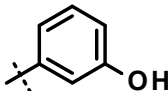
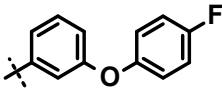
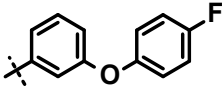


24
25 **Figure 1** The structure of some recently disclosed potent and selective Mcl-1 inhibitors with reported
26 *in vivo* efficacy
27
28
29
30

31 Results

32
33 Fragment screening against Mcl-1 and Bcl-2 identified a number of carboxylic acid containing
34
35 compounds from which the thienopyrimidine derivative **1a** emerged as a hit. This compound
36
37 showed comparable affinity against both targets (K_i of 50 μ M and IC_{50} of 164 μ M respectively) while
38
39 being moderately selective vs Bcl-x_L (Table 1). The near neighbour screen of analogues (**1b-1g**)
40
41 convincingly validated this series as a starting point for hit expansion. Replacing the ethyl group by a
42
43 phenyl (**1b**) in the 5 position maintained the Mcl-1 affinity while increased selectivity against Bcl-2.
44
45 The same was also true for substituted phenyl analogues **1c** and **1d**. Interestingly the para
46
47 substituted analogue (**1c**) had decreased selectivity towards Bcl-x_L. The *m*-hydroxyphenyl analogue
48
49 with a reversed amino acid stereochemistry (**1e**) showed also very similar affinity towards Mcl-1
50
51 while its affinity towards Bcl-2 increased considerably. Increasing the size of the 5 substituent (**1f-g**)
52
53 was also well tolerated both by Mcl-1 and Bcl-2 and the observed affinity values were also
54
55 corroborated by orthogonal techniques (Table 1).
56
57
58
59
60

Table 1. Mcl-1, Bcl-2, Bcl-x_L inhibition of early thienopyrimidine hits (**1a-g**)

	R	AA	Mcl-1 ¹	Bcl-2 ¹	Bcl-x _L ¹
1a	Et	S-Me	50	74	NM
1b		S-Me	110	418	NM
1c		S-Me	44	359	216
1d		S-Me	21	437	NM
1e		R-Me	45	5.0	60%@2.5mM
1f		S-Me	130	98	33
1g		R-Me	19 ^{2,3}	6.1 ²	50%@1mM

¹ K_i measured in Mcl-1, Bcl-2 or Bcl-x_L FP assay in μM unless incomplete assay curve. NM – not measurable at the concentrations used in the assay (2.5 mM or solubility limit)

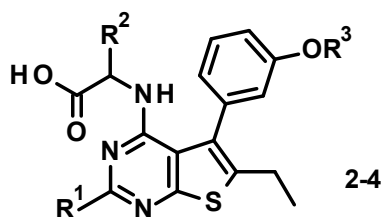
² For K_d measured by HSQC NMR assay see Supporting Information

³ For K_d measured by ITC assay see Supporting Information

1
2
3 Having validated the thienopyrimidines as a fragment hit series, in the absence of structural
4 guidance we embarked on the systematic variation of the core substituents. The analysis of the
5 binding data obtained on a small set of analogues revealed that modifications in the 2 position were
6 well tolerated but led to a substituent dependent selectivity profile. The smaller methylsulfonyl (**2a**)
7 derivative maintained affinity for Mcl-1 and also gained comparable affinity for Bcl-x_L while showing
8 a minor drop in affinity for Bcl-2. On the other hand the pyridyl (**2b**) and sulfonamidophenyl (**2c**)
9 derivatives were more efficient inhibiting Bcl-2 than Bcl-x_L (Table 2).

10
11
12
13
14
15
16
17
18
19
20
21 The variation of the amino acid substituent in the 4 position (**3a-e**) was also well tolerated. There
22 was no clear preference for any of the targets and the chirality of the side chain seemed to have only
23 minor influence on the affinity. Changing alanine to serine (**3a**) had no effect on binding to Mcl-1 but
24 modified selectivity towards the other targets. The phenylglycine analogue **3b** brought affinity down
25 to the mid-micromolar range for all three targets. The influence of the chirality on the strength and
26 selectivity of the binding was explored with the phenylalanine derivatives **3c** and **3d**. Variation of the
27 absolute stereochemistry had little or no effect on the affinity or selectivity, both compounds
28 showing a similar profile as **3b**. The saturated analogue **3e** behaved very similarly to its parent
29 compound **3c**.

30
31
32
33
34
35
36
37
38
39
40
41
42
43 For comparison we have also synthesized some analogues that bear the 3-hydroxyphenyl
44 substituent in position 5 (**4a-d**). The *R*- (**4a**) and *S*-phenylglycine (**4b**) analogues behaved similarly
45 showing a mild target dependent preference for one or the other stereoisomer. Comparing with the
46 more developed **3b** we observed a similar selectivity profile but a considerable (ca. 10-fold)
47 improvement of affinity against all targets. The stereochemistry of the amino acid moiety had little
48 effect – as already seen for **3c-3d**. The trends were slightly different for the *R*- (**4c**) and *S*-
49 phenylalanine (**4d**) analogues. Although both enantiomers showed similar affinities and selectivity
50 profile, in comparison with **3c** and **3d** we observed an increased selectivity towards Mcl-1.
51
52
53
54
55
56
57
58
59
60

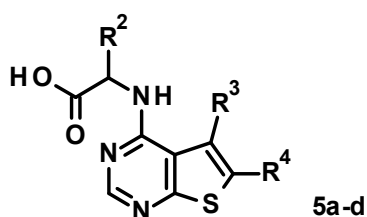
Table 2. Mcl-1, Bcl-2, Bcl-x_L inhibition of thienopyrimidine derivatives **2-4**

	R ¹	R ²	R ³	Mcl-1 ¹	Bcl-2 ¹	Bcl-x _L ¹
2a		<i>R</i> -Me	4-fluorophenyl	44	51	26
2b		<i>R</i> -Me	4-fluorophenyl	8.4	4.1	18
2c		<i>R</i> -Me	4-fluorophenyl	50	1.3	39
3a	H	<i>rac</i> -CH ₂ OH	4-fluorophenyl	61	71%	87
3b	H	<i>rac</i> -Ph	4-fluorophenyl	68	13	15
3c	H	(<i>R</i>)-Bn	4-fluorophenyl	51	24	24
3d	H	(<i>S</i>)-Bn	4-fluorophenyl	77	24	18
3e	H	(<i>R</i>)-CH ₂ Cy	4-fluorophenyl	53	8.1	17
4a	H	(<i>R</i>)-Ph	H	7.7	470	319
4b	H	(<i>S</i>)-Ph	H	27	269	107
4c	H	(<i>R</i>)-Bn	H	10	63%	75%
4d	H	(<i>S</i>)-Bn	H	58	68%	73%

¹ K_i measured in Mcl-1, Bcl-2 or Bcl-x_L FP assay in μM (or % inhibition at 1 mM if incomplete assay curve)

In the next step we assessed the effect of 6-substituents on the affinity and selectivity of our compounds (Table 3). The absence of a substituent (**5a**) or the introduction of a phenyl group (**5b**) were both tolerated, although the latter compound was more potent and showed less selectivity towards Bcl-2. Further introduction of a benzene moiety on the amino acid (**5c**) showed no significant effect. Returning to the ethyl substituent in the 6-position and replacing the phenol in the 5-position by a 2-naphthyl moiety (**5d**) had no beneficial effect on the affinity or selectivity of the molecule but we were able to obtain structural information about the binding of our compounds for the first time using an NMR guided model.

Table 3 Mcl-1, Bcl-2, Bcl-x_L inhibition of thienopyrimidine derivatives **5a-d**



	R ²	R ³	R ⁴	Mcl-1 ¹	Bcl-2 ¹	Bcl-x _L ¹
5a	<i>R</i> -Me	3-hydroxy-phenyl	H	59 ²	4%@2.5mM	287
5b	<i>R</i> -Me	3-hydroxy-phenyl	Ph	27 ²	49	42
5c	<i>R</i> -Bn	3-hydroxy-phenyl	Ph	24	21	71%@1mM
5d	<i>R</i> -Me	2-naphthyl	Et	110 ²	29%@2.5mM	20%@2.5mM

¹ K_i measured in Mcl-1, Bcl-2 or Bcl-x_L FP assay in μM or percentage inhibition at top concentration if incomplete assay curve.

² For K_d measured by HSQC NMR assay see Supporting Information

1
2
3 ***First structural insight – NMR Guided Model established for 5d in Mcl-1***
4

5 The NOE distance constraints suggested that compound **5d** is in contact with Mcl-1 via the naphthyl
6 ring and one of the two methyls (from either the 2- or 6- position). The residues giving rise to the
7 NOEs are indicated in Figure 2a. In Figure 2b, the surface of Mcl-1 is coloured in yellow to show
8 where the NOEs occurred. This suggests that compound **5d** binds to a location similar to which
9 Leu10 and Ile13 (red sticks) from the bound Bim peptide (red tube) occupy.
10

11 Analysis of the available BH3 public structures at the beginning of this work already suggested a
12 significant conformational change between a peptide-bound to a compound-bound BH3 protein. Yet
13 when we started to work on compound **5d** binding model, there were only peptide-bound Mcl-1
14 structures. To address the possibility of protein flexibility, a protein conformational ensemble was
15 prepared for Mcl-1 to model compound **5d**. When enumerating such ensemble of conformations,
16 we focused particularly on the residues involved in the NOEs. Compound **5d** was then docked into all
17 enumerated protein conformations. The resulting docking models were visually inspected and the
18 best three docking models in terms of satisfying the observed NOEs were then subjected to induced-
19 fit docking protocol. This was to further explore the complementarity between the compound **5d**
20 and hypothesized Mcl-1 conformation.¹⁴ And this led to a final model shown in Figure 2c, with the
21 ethyl and naphthyl ring in close contact with Mcl-1 and the acid likely pointing towards the solvent.
22 The proposed binding mode is in line with most of the observed SAR (e.g. 2-position, 6-position) but
23 the observed Mcl-1 selectivity for **4c** and its analogues is difficult to interpret. Of note is that the
24 final NGM starting from peptide-bound Mcl-1 structures deviates from the X-ray structures obtained
25 at a later stage of the project despite efforts made to explore the protein flexibility. Nevertheless,
26 the NGM offers a number of hypotheses to be tested.
27
28
29
30
31
32
33
34
35
36
37
38
39
40
41
42
43
44
45
46
47
48
49
50
51
52
53
54
55
56
57
58
59
60

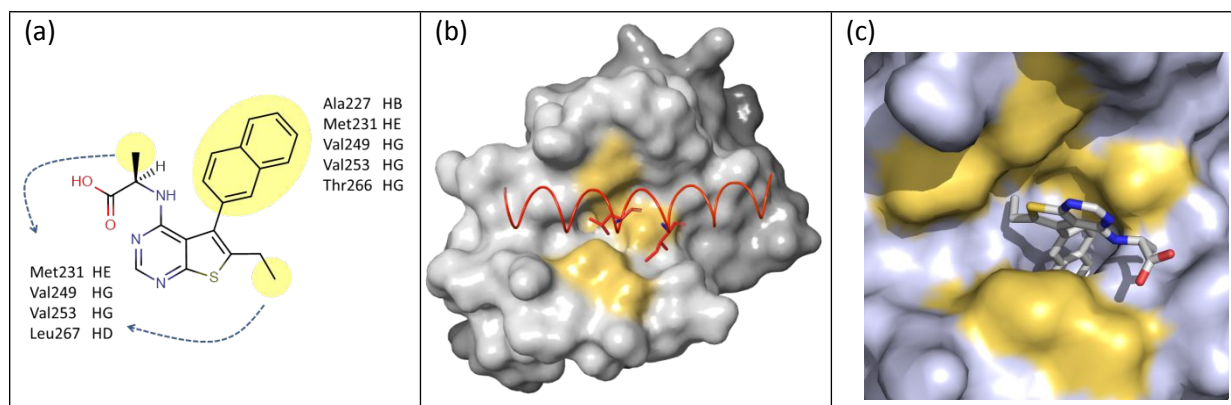


Figure 2. NMR guided model of **5d**. The observed NOEs between Mcl-1 and **5d** are summarized in

(a). The broken arrows suggest that either of the methyls could contribute to the observed NOEs. (b)

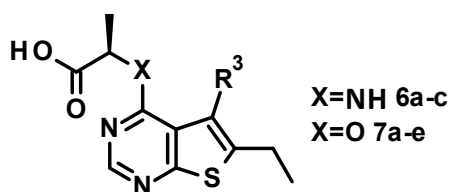
The NOEs highlighted in yellow surface are mapped to the Bim-bound Mcl-1 (2PQK) in grey surface.

The Bim is shown in red tube with Leu10 and Ile13 highlighted in red sticks. (c) The final binding

model of **5d** is shown in with yellow surface indicating the residues giving rise to the NOEs.

With the structural guidance in hand we set out to explore the limits and flexibility of the hydrophobic S2 pocket. Fixing the 6-position substituent as ethyl to allow for some flexibility within the pocket and staying with alanine in the 4-position first we evaluated the 5-indolyl derivative **6a**. This compound showed good affinity towards both Mcl-1 and Bcl-2, which was also verified by orthogonal techniques. The replacement of the linking nitrogen atom of the amino acid by oxygen (**7a**) improved Mcl-1 binding by 6-8 fold. Since aryl ethers have a different rotational barrier than the one from anilines, it would seem that the ether oxygen may offer a more preferable torsional profile for Mcl-1 binding, its bioactive torsion well aligned with its energy minimum. Changing the polarity and flexibility of the 5-substituent by replacing indolyl with 2-naphthyl (**7b**) or *p*-isopropylphenyl (**7c**) was also well tolerated resulting only in a minor drop of affinity. Probing the flexibility of the system we also prepared the *o*-benzyloxyphenyl derivative in the amino acid series (**6b**). In the reaction a mixture of diastereoisomers was formed that were separable and we isolated **6b** as the later eluting diastereoisomer. This compound has also maintained its affinity towards Mcl-1 hinting that through a conformational mobility Mcl-1 might accommodate bulky but flexible *ortho*-substituents on the

1
2
3 aromatic ring. **6b** showed a high selectivity against the other targets therefore in the next set of
4
5 compounds we introduced the *o*-tolyl moiety in the 5-position. These molecules also possess
6
7 hindered rotation around the biaryl axis and their atropoisomers might be separated. We have
8
9 isolated and tested the pair of diastereomeric compounds **7d** and **7e**, which showed very similar
10
11 affinity towards Mcl-1. The relative stereochemistry of the atropoisomers was not determined. The
12
13 amino acid analogue **6c** was tested as a 3:7 mixture of atropoisomers and showed a comparable
14
15 affinity as the hydroxyl acid analogues. All the *o*-tolyl analogues (**7d-e,6c**) inherited the
16
17 advantageous selectivity profile of **6b**.
18
19
20
21
22
23
24
25
26
27
28
29
30
31
32
33
34
35
36
37
38
39
40
41
42
43
44
45
46
47
48
49
50
51
52
53
54
55
56
57
58
59
60

Table 4 Mcl-1, Bcl-2, Bcl-x_L inhibition of thienopyrimidine derivatives **6-7**

	R ³	X	Mcl-1 ¹	Bcl-2 ¹	Bcl-x _L ¹
6a		NH	22 ^{2,3}	28 ²	67%@2.5mM
7a		O	2.8	NM	10%@0.33mM
7b		O	6.0	NM	57%@1mM
7c		O	8.1	NM	41%@1mM
6b		NH	24	20%@2.5mM	27%@2.5mM
7d		O	18	NM	25%@1mM
7e		O	15	NM	34%@1mM
6c		NH	100	70%@1mM	4%@1mM

¹ K_i measured in Mcl-1, Bcl-2 or Bcl-x_L FP assay in μM unless incomplete assay curve. NM – not measurable at the concentrations used in the assay (2.5 mM or solubility limit)

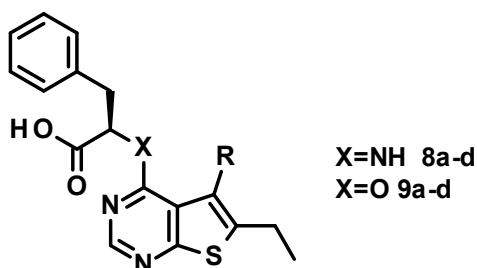
² For K_d measured by HSQC NMR assay see Supporting Information

³ For K_d measured by ITC assay see Supporting Information

At this point we also obtained the X-ray structures of the 2-indolyl analogues both in the amino (**6a**) and hydroxy (**7a**) acid series (Figure 3). In both structures (**6a** and **7a**) the 2-indolyl moiety points

1
2
3 towards the solvent, with Met231 just ~4Å away from the side of the ring. The indolyl ring is ~56 (**7a**)
4 to 58 (**6a**) degrees rotated from the thienopyrimidine's plane, fitting into the groove between
5
6 Ala227 and Met231. Analysis of this newly revealed binding mode suggested that major
7
8 improvements could be achieved by the fine tuning of the amino/hydroxyl acid side chain and the 5-
9
10 substituent. *D*-phenylalanine was already shown to have a beneficial effect both on the affinity and
11
12 selectivity (*e.g.* **4c**). Combining this feature with the 4-indolyl moiety in the 5-position gave separable
13
14 diastereoisomers **8a** and **8b** and we observed submicromolar affinity for the first time (confirmed by
15
16 ITC) and a high selectivity towards Mcl-1. The atropoisomers were only mildly differentiated. The
17
18 hydroxyl acid analogues **9a** and **9b** behaved alike with 490 and 640 nanomolar IC₅₀s respectively. The
19
20 X-ray structures of **8a** and **8b** revealed (Figure 3) that the pocket can accommodate both
21
22 atropoisomers similarly. All major elements (*e.g.* the phenyl side chain, the thienopyrimidine core,
23
24 the ethyl core substituent, and the indole moiety) occupy the same space in the two structures,
25
26 which explains the similar observed affinity of the diastereoisomers. Based on earlier observations
27
28 the *o*-tolyl analogues were expected to show a similar behaviour. The respective diastereomers were
29
30 synthesized and tested in both the amino acid (**8c-d**) and hydroxyl acid (**9c-d**) series. For both pairs
31
32 of compounds we observed a more pronounced difference of affinity between the atropoisomers
33
34 the more active ones registering around 1 μM. The X-ray structure of the more active stereoisomer
35
36 **8d** in the bound form (Figure 3) was coherent with the previous structures and it revealed that the
37
38 methyl group points towards the protein forming hydrophobic contacts with Phe228 and Phe270.
39
40 Such hydrophobic contacts could explain the affinity difference between atropoisomers as the other
41
42 atropoisomer (**8c**) would lose such favourable interaction by projecting the methyl towards the
43
44 solvent leading to weaker affinity. We have investigated the stability of the atropoisomers and found
45
46 no interconversion by ¹H NMR on heating the solution of **8d** in deuterated dimethylsulfoxide at 373
47
48 K for 30 mins. This finding ensured that the interconversion of **8c-8d** or **9c-9d** doesn't bias our
49
50 biophysical measurements at ambient temperature.
51
52
53
54
55
56
57
58
59
60

Table 5 Mcl-1, Bcl-2, Bcl-x_L inhibition of thienopyrimidine derivatives showing atropoisomerism in the 5-position (8-9)



	R	X	Isomer ³	Mcl-1 ¹	Bcl-2 ¹	Bcl-x _L ¹
23	8a	NH	1	1.6 ²	70%@1mM	135
26	8b	NH	2	5.7 ²	77%@1mM	76%@1mM
27						
28	9a	O	1	0.49 ²	NM	NM
29						
30	9b	O	2	0.64 ²	11%@10μM	NM
31						
32	8c	NH	1	58	14%@1mM	4%@1mM
33						
34	8d	NH	2	2.4 ²	46%@1mM	22%@1mM
35						
36	9c	O	1	3.4	NM	NM
37						
38	9d	O	2	0.89	5%@10μM	2%@10μM
39						

¹ K_i measured in Mcl-1, Bcl-2 or Bcl-x_L FP assay in μM unless incomplete assay curve. NM – not measurable at the concentrations used in the assay (10 μM or solubility limit)

² For K_d measured by ITC assay see Supporting Information

³ arbitrary assignment of diastereomers based on the chromatographic elution order

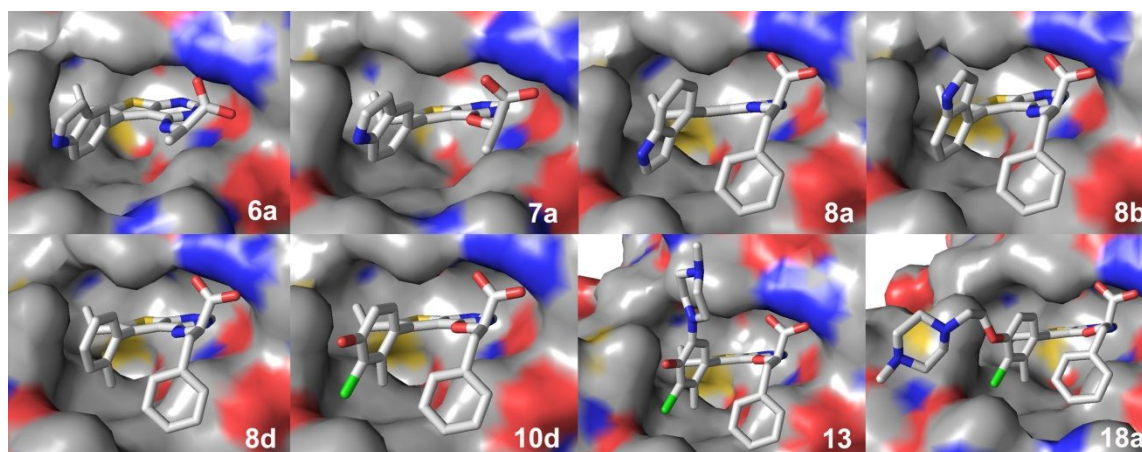


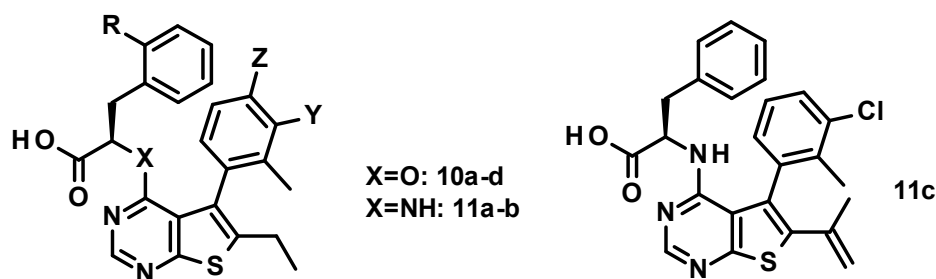
Figure 3. Crystal structures of compounds **6a** (PDB code 6QXJ), **7a** (6QYK), **8a** (6QZ5, 6QYL), **8b** (6QZ6, 6QZ7), **8d** (6QZB), **10d** (6QZ8, 6QYN), **13** (6QYP), and **18a** (6QYO) bound to the S2 pocket of Mcl-1.

Structure determination details can be found in the supplementary material.

The bound structure of **8d** suggested that we might pick-up further interaction with the protein backbone (Ala227) by introducing a chlorine or bromine next to the methyl group. The 4-position of the same benzene ring also offers a vector for projecting substituents towards the solvent (i.e. to improve compound properties). The introduction of bromine onto **9c** and **9d** resulted in the atropisomers **10a** and **10b** respectively. The stereoisomer **10a** showed very similar affinity to its parent **9c**, which is understandable considering that the bromine and the methyl group are projected towards the middle of the pocket. In contrary the affinity of the isomer **10b** was improved suggesting that the bromine atom might pick up some interaction with the protein. Using the more compact chlorine instead of the bromine (**10c**) was also well tolerated. As expected this halogenated compound maintained the selectivity towards other family members. The affinity of the amino acid analogue **11a** was in the same range both by FP and ITC assays.

To further improve the affinity for Mcl-1 we assessed two approaches based on the available structural information. First we prepared the 2-methoxy-*D*-phenylalanine analogue **11b**. As expected this modification was well tolerated showing very similar affinity and selectivity as the parent compound (**11a**). The other modification was the replacement of the ethyl moiety with a 2-propenyl

1
2
3 group (**11c**). The resulting compound showed unfortunately no improvement but maintained more
4
5 or less the affinity of the ethyl analogue. Finally we have tested the applicability of the benzene ring
6
7 in position 5 as a starting point towards the solvent. The introduction of the phenolic function (**10d**)
8
9 was not only tolerated but led to a significantly improved affinity for the target that was also
10
11 validated by orthogonal techniques. We also determined the bound structure of **10d** (Figure 3),
12
13 which confirmed that the phenolic hydroxyl group should be a suitable vector towards the solvent.
14
15
16
17
18
19
20
21
22
23
24
25
26
27
28
29
30
31
32
33
34
35
36
37
38
39
40
41
42
43
44
45
46
47
48
49
50
51
52
53
54
55
56
57
58
59
60

Table 6 Mcl-1, Bcl-2, Bcl-x_L inhibition of the advanced thienopyrimidine derivatives **10-11**.

	Y	Z	R	Isomer ³	X	Mcl-1 ¹	Bcl-2 ¹	Bcl-x _L ¹
10a	Br	H	H	1	O	5.3	NM	NM
10b	Br	H	H	2	O	0.33 ²	NM	NM
10c	Cl	H	H		O	0.81	36	62%@0.2mM
11a	Cl	H	H	1	NH	0.51 ²	29	48%@0.2mM
11b	Cl	H	Ome	2	NH	0.26 ²	38%@0.2mM	11%@0.2mM
11c	Cl	H	H		NH	19	5.4	35%@0.5mM
10d	Cl	OH	H		O	0.051 ²	61%@0.2mM	29%@0.2mM

¹ K_i measured in Mcl-1, Bcl-2 or Bcl-x_L FP assay in μM unless incomplete assay curve. NM – not measurable at the concentrations used in the assay (10 μM or solubility limit)

² For K_d measured by ITC assay see Supporting Information

³ arbitrary assignment of diastereomers based on the chromatographic elution order

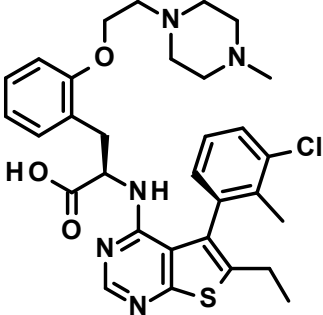
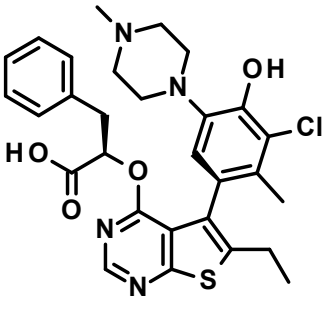
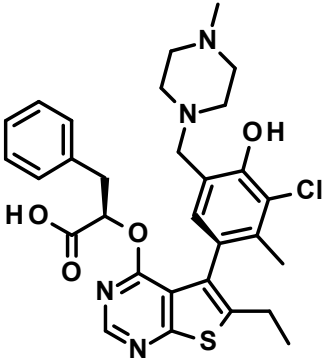
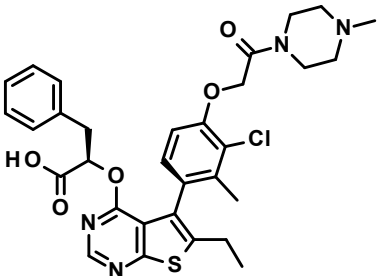
With the affinity of our compounds for Mcl-1 reaching the low nanomolar range we set-up cellular viability assays in the H929 multiple myeloma cell line, an MCL1-dependent cell line¹² as single agent or in combination with ABT-263, which sensitizes H929 cells through the inhibition of other important anti apoptotic proteins (Bcl-2, Bcl-x_L, Bcl-w). To assess and mitigate the potential limiting effect of plasma protein binding, some of the cellular assays were also run both at standard (10%) and lower (0.1%) serum concentrations. Our compounds (*e.g.* **10d**, **11b**) showed no cellular activity,

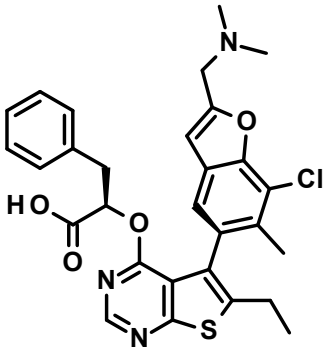
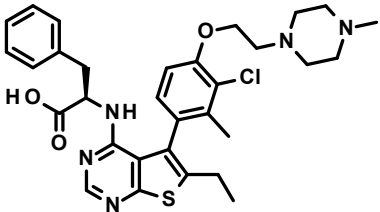
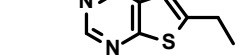
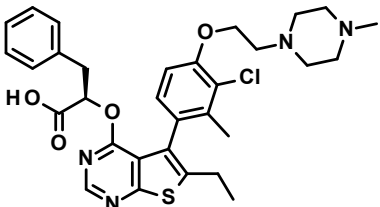
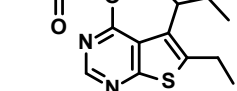
1
2
3 which we linked to poor anticipated cellular penetrance. In order to improve this property we
4 explored the introduction of a basic group onto our molecules. This modification was expected to
5 offset the negative charge of the carboxylate group under physiological conditions. On analysis of
6 the bound structure of **10d** (Figure 4), we concluded that this additional moiety could be introduced
7 either into the *ortho*-position of the benzene ring on the amino/hydroxyl acid or on the tolyl moiety
8 in the 5-position.
9

10 Our selected permeabiliser, the methylpiperazine moiety was first connected to **11b** using a two
11 carbon linker (**12**). In spite of a significant loss of affinity (0.36 μM *cf.* 0.024 μM by ITC) **12** registered
12 in our viability assays. Its IC_{50} of 20.3 μM under standard conditions was slightly improved both by
13 the addition of ABT-263 (12 μM) and by the decrease of the serum concentration in the experiment
14 to 0.1% (9.8 μM ; single agent). Using the tolyl moiety as the anchoring point and connecting the
15 piperazine to its 5-position either directly (**13**) or through a methylene linker (**14**) resulted in the
16 same beneficial effect. We have obtained the X-ray structure of **13** bound to Mcl-1 (Figure 3), which
17 showed that the piperazine moiety is nicely accommodated in the solvent exposed part of the
18 binding pocket and it has not changed the way the ligand is bound. Both **13** and **14** registered in the
19 cellular assays as single agent under standard conditions (13.3 μM and 15.5 μM at 10% serum) and
20 this effect was attenuated in combination with ABT-263 (4.2 μM and 5.4 μM respectively). Using the
21 phenolic hydroxyl group of **10d** as an anchor point and linking it through an acetyl moiety (**15**) was
22 also very well tolerated. The observed affinity was again very similar to the parent phenol while the
23 compound registered in the cellular assays in the low micromolar range. The tolerance of the
24 substitution of both the 4- and 5-positions of the tolyl moiety suggested that cyclization of the two
25 positions should also be tolerated. Indeed the benzofurane analogue **16** showed comparable
26 characteristics to its "parents" **14** and **15** both affinity wise and considering its cellular activity.
27 Finally we have incorporated a simple ethylene linker to connect the N-methylpiperazine moiety to
28 the phenolic oxygen. Of this compound both the amino acid (**17**) and the hydroxyl acid (**18**)
29 analogues were prepared.
30
31
32
33
34
35
36
37
38
39
40
41
42
43
44
45
46
47
48
49
50
51
52
53
54
55
56
57
58
59
60

1
2
3 To better understand the behaviour of these compounds and their biological effect, we isolated and
4 tested both atropoisomers (**17a-b**, **18a-b**). Comparing the amino (**17a**) and hydroxyl (**18a**) acids the
5 latter showed both superior affinity towards Mcl-1 and more efficient cell killing in the viability
6 assay. As expected the atropoisomeric compounds **17b** and **18b** showed a significantly decreased
7 affinity for Mcl-1, which made them good controls in the following pharmacological studies. The
8 absolute configuration of **18a** was also confirmed by determination of the structure of its Mcl-1
9 bound complex (Figure 3), which showed that the methyl group and the chlorine atom interact with
10 the protein surface while the piperazine unit is projected towards the solvent as expected. This
11 proved that the para position (Z in Table 6) of the 5-phenyl moiety is able to modulate physical
12 properties and cellular activities of the series, while maintaining the same mode of binding.
13
14
15
16
17
18
19
20
21
22
23
24
25
26
27
28
29
30
31
32
33
34
35
36
37
38
39
40
41
42
43
44
45
46
47
48
49
50
51
52
53
54
55
56
57
58
59
60

Table 7. Mcl-1 inhibition and cell killing of thienopyrimidine derivatives (**12-18**) in the presence and absence of ABT-263

Structure	Mcl-1 ¹	MTT w ABT-263 IC ₅₀ ²	MTT IC ₅₀ ³
	2.0 ⁴	12.2	20.3/9.8
	0.046 ⁴	4.2	13.6/4.7
	0.032 ⁴	5.4	15.5/NA
	0.021 ⁴	6.9	17.1/NA

16		0.076 ⁴	10	20.4/3.8
17a		0.22 ⁴	2.5	11.6/1.7
17b		170	--	>30μM/>30μM
18a		0.019 ⁴	1.1	5.6/1.0
18b		25	23.4	27.2/NA

¹ K_i measured in Mcl-1 FP assay in μM

² IC₅₀ measured in cell viability assay in μM in H929 cells following 48h incubation in the presence of 1 μM ABT-263.

³ IC₅₀ measured in cell viability assay in μM in H929 cells following 48h incubation in the presence of 10%/0.1% serum.

⁴ For K_d measured by ITC and SPR assay see Supporting Information

The finding that **18a** inhibits Mcl-1 and induces cell death when used as single agent in H929 cancer cells at single digit micromolar level prompted us to probe its behaviour in more detail. To ensure that we have a real Mcl-1 binder we ran two different binding assays with Mcl-1. In the ITC experiment we measured a K_d of 30 nM, while in an SPR experiment with immobilized Mcl-1 we observed a K_d of 10 nM with a dissociation half-life of 17.5 second. Both of these data align well with the K_i of 19 nM measured in the primary FP assay.

1
2
3 The next experiment aimed at proving that **18a** acts in cells through displacing selectively a relevant
4 proapoptotic BH3 domain containing protein from its Mcl-1 complex. To this end, HeLa cells
5 overexpressing Flag-Mcl-1 or Flag-Bcl-xL were treated with different doses of **18a** and **18b**. Following
6 immunoprecipitation using anti-Flag antibody, the endogenous Bak protein complexed with either
7 Mcl-1 or Bcl-xL was monitored (Figure 4a). Interestingly, the Mcl-1/Bak complex was disrupted
8 following treatment with compound **18a**, as evidenced by the dose-dependent decrease of
9 endogenous Bak co-immunoprecipitated with Flag-Mcl-1. In the same conditions, no effect was
10 observed on the Bcl-xL/Bak complex. As negative control, treatment with its corresponding less
11 active atropoisomeric compound **18b** did not affect the Mcl-1-Bak complex.

12 Selective Mcl-1 inhibitors were reported to stabilize the level of endogenous Mcl-1 protein in a dose-
13 dependent manner.^{11a,12a, 12b} To monitor this target hitting, colon carcinoma HCT116 cell line (not
14 sensitive to Mcl-1 inhibition^{12a}) was treated with different doses of Mcl-1 inhibitors **17a** and **18a** and
15 their corresponding less active diastereoisomers **17b** and **18b**. Significant dose-dependent increase
16 of the endogenous Mcl-1 protein was observed following treatment with either compound **17a** or
17 **18a** (Figure 4b). Interestingly, this assay is clearly more sensitive than the viability assay since the
18 two active compounds exhibited activity at doses as low as 0.3 μ M. The lack of concomitant PARP-
19 cleavage confirmed the absence of apoptosis induction in this cell line resistant to Mcl-1 inhibition.
20 Importantly, the less active atropoisomers (**17b**, **18b**) exhibited no effect on the Mcl-1 protein level
21 thus further supporting Mcl-1 target hitting with active compounds (**17a** and **18a**) in cells.
22
23
24
25
26
27
28
29
30
31
32
33
34
35
36
37
38
39
40
41
42
43
44
45
46
47
48
49
50
51
52
53
54
55
56
57
58
59
60

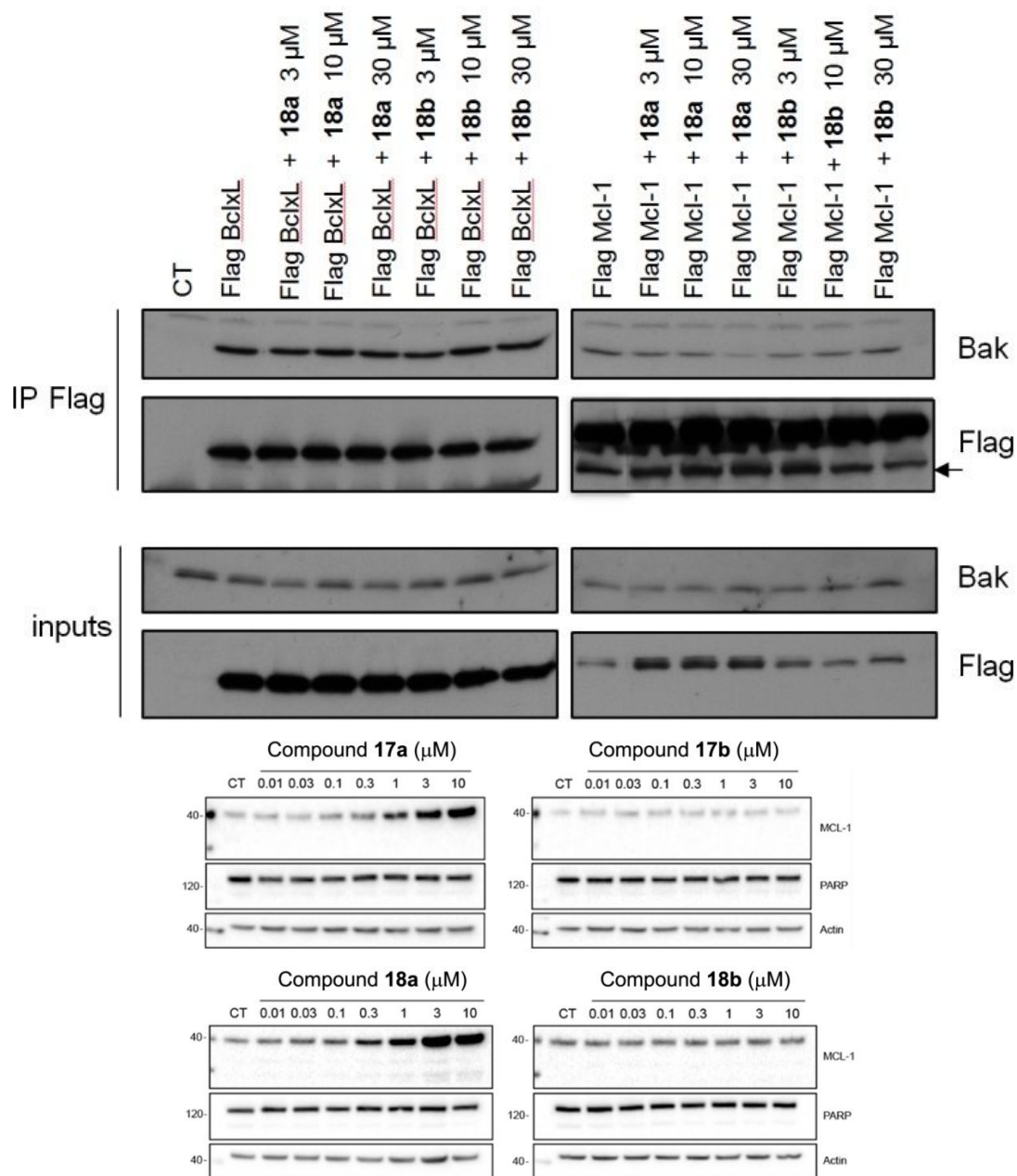


Figure 4. a) Evaluation of Mcl-1 inhibitors on Mcl-1/Bak and Bcl-xL/Bak complexes by co-immunoprecipitation; Arrow indicates Flag-MCL-1; b) Dose-dependent Mcl-1 stabilisation in HCT116 cells following treatment with **17a** and **18a** compounds and their less active diastereoisomers (**17b**, **18b**).

Once Mcl-1 target hitting was demonstrated with compounds **17a** and **18a**, we next asked whether these Mcl-1 inhibitors could induce apoptosis in a Mcl-1 sensitive cell line. To this end, H929 multiple myeloma cell line was treated for 6h with different doses of **17a**, **17b**, **18a**, and **18b** in the presence

or absence of ABT-263, which was expected to further sensitize cells to Mcl-1 inhibition. Two different but commonly accepted apoptotic cellular readouts were used: PARP cleavage and cleaved Caspase-3. As shown in Figure 5, **17a** and **18a** induced both PARP and Caspase-3 cleavage in this cell line in a dose-dependent manner. This effect was amplified by the addition of the Bcl-2/Bcl-x_L inhibitor ABT-263 and completely abrogated by the caspase inhibitor Q-VD-Oph (QVD). Importantly, the less active diastereomers showed no apoptosis induction, in agreement with our previous findings. Altogether, these data suggest that **17a** and **18a** are selective Mcl-1 inhibitors capable of demonstrating on-target cell killing in H929 cancer line through activation of the apoptotic pathway.

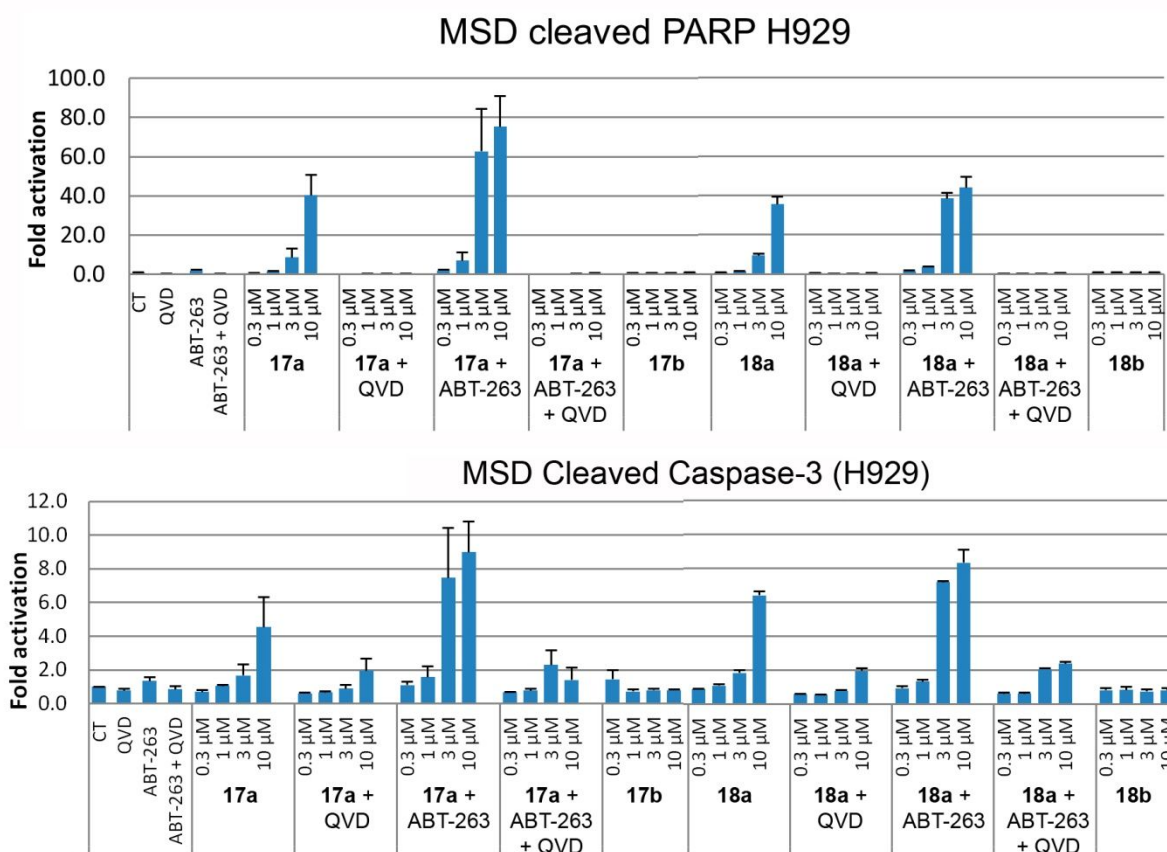


Figure 5. Dose-dependent apoptosis induction in H929 cells following treatment with Mcl-1 inhibitors **17a** and **18a** and their less active diastereoisomers (**17b**, **18b**) in the presence or absence of ABT-263 and caspase inhibitor QVD.

Based on their affinity and cellular activity, ADME properties of **17a** and **18a** were further characterized. Their hepatic microsomal clearance in mice or rat was good to acceptable with a clear superiority of **18a** (Table 8, 30 and 11 ml/min/kg vs 72 and 23 ml/min/kg respectively). In the presence of human microsomes **18a** was also less metabolised than **17a** (10 vs 18 ml/min/kg) although both values were inferior compared to the rodent species. As it is typical for PPI inhibitors¹⁵ both compounds have a very low free fraction in plasma (**18a**: 0.2% in mice and 0.5% in human vs 0.2% and 0.2% for **17a** respectively). The stability of **17a** and **18a** in the presence of hepatocytes without added plasma was low for human (18 and 17 ml/min/kg) while acceptable to good for mice (75 and 9 ml/min/kg) and rat (42 and 20 ml/min/kg) showing again a superiority of the hydroxyl acid. As one might expect from the high PPB values the metabolic clearance of both **17a** and **18a** became good in hepatocytes in the presence of added plasma (mice: 3 and 0 ml/min/kg, rat: 24 and 0 ml/min/kg, human: 0 and 5 ml/min/kg). The predicted human intestinal absorption of **17a** and **18a** in the Caco-2 model were 59% and 29% with mass recoveries at 82% and 77%, respectively.

	human				mice			rat	
	CL pred (ml/min/kg)		FU(%)	Fabs(%)	CL pred (ml/min/kg)		FU(%)	CL pred (ml/min/kg)	
	MIC	HEP			MIC	HEP		MIC	HEP
17a	18	18/0 [#]	0.2	59	72	75/3 [#]	0.2	23	42/24 [#]
18a	10	17/5 [#]	0.5	29	30	9/0 [#]	0.2	11	20/0 [#]

Table 8. In vitro ADME parameters of **17a** and **18a** (MIC-microsomes, HEP-hepatocytes). #- experiment run with added plasma

To test the predictive power of the in vitro ADME data, *in vivo* PK studies were also run in mice. The compounds (**17a**, **18a**) were dosed 1 mpk i.v. and 3 mpk p.o. On i.v. administration, both compounds showed a similar profile (Table 9) while **18a** was more persistent than **17a** as manifested in the

different PK parameters. This finding is in line with the difference in metabolic stability observed *in vitro*, although the clearance of **17a** was higher than one would estimate based on hepatocyte data. The *in vitro* data suggested that the difference between **17a** and **18a** exposure would be levelled on oral dosing, which was indeed the case. The calculated oral bioavailabilities were 16% and 9% respectively which indicated limited absorption as suggested by *in vitro* Caco-2 results.

	i.v. 1mpk					p.o. 3mpk			F%
	t _{1/2} h	Cl plasma mL/min/kg	AUC _t ng/mL.h	V _d L/kg	blood/ plasma ratio	C _{max} ng/mL	t _{1/2} h	AUCt ng/mL.h	p.o./ i.v.
17a	0.65	33	509	0.9	0.7	64	3.8	168	16%
18a	3.7	5.7	2863	1.0	0.6	199	1.7	781	9%

Table 9. *in vivo* PK parameters of **17a** and **18a** in mice.

To assess the drug-drug interaction and off-target profile of our leads, potential inhibitory effect of these compounds was evaluated on 5 different human CYP450 enzymes (3A4, 2D6, 1A2, 2C9, 2C19). **17a** inhibited only CYP 3A4 with an IC₅₀ of 5.2 μM while the IC₅₀ of **17a** or **18a** against the remaining enzymes was not reached until 20 μM. **18a** was also submitted to an hERG patch-clamp assay and showed a dose-dependent inhibition reaching 28% at 10 μM concentration. Neither a safety receptors profile nor *in silico* genotoxicity assessment of **18a** showed any alerts. Based on these data, **18a** appeared as a promising lead compound ready for more extended optimization.

Discussion and Conclusions

An NMR-based fragment screen identified thieno[2,3-*d*]pyrimidines bearing an amino acid in the 4-position and a small alkyl substituent in the 6-position as an interesting, non-selective hit for Mcl-1. A systematic variation of the available positions and use of orthogonal assays confirmed the hit series and allowed the initiation of a fragment growing program. In the early stages, varying selectivities were observed and typically Mcl-1 and Bcl-2 were inhibited alike. Structural guidance was provided by NMR-guided model building and later by X-ray crystallography. It is interesting to note that the presence of different binding modes was observed at this stage of the development. A significant breakthrough came with the introduction of such aromatic substituents into the 5-position of the thienopyrimidine core that showed restricted rotation due to the presence of an *ortho*-substituent. These molecules were highly selective for Mcl-1 and affinities shifted to the sub-micromolar range. Structure-guided fine-tuning of the inhibitors and the introduction of a basic nitrogen into the solvent exposed part of the molecule to offset the charge of the carboxylic acid under physiological conditions led to potent and selective inhibitors which induced cell killing. Cellular efficacy was observed in correlation with the expected mechanism-based events such as Mcl-1 stabilization, caspase induction and PARP cleavage. The combined data of cellular experiments suggest that to induce apoptosis in Mcl-1 dependent cell lines significant higher doses than the K_d of the inhibitor are required, which is probably linked to the need of replacing most of the BH3-only proapoptotic proteins from their complex with Mcl-1. The pharmacokinetic properties of the lead compounds were determined as well as any potential DDI liability. Since favourable results were obtained in all assays, these lead compounds were further developed leading to the discovery of anti-Mcl-1 clinical candidate.

Experimental section

General

1
2
3 All obtained products had an LC purity above 96% that was corroborated by their ¹H NMR spectrum
4
5 unless specifically mentioned otherwise. All synthetic experimental details including the
6
7 characterisation of the compounds are described in the Supporting Information.
8
9

10 **Pharmacology material and method**

11
12 **Compounds.** ABT-263 was purchased from Selleck-chem and QVD-OPh from Sigma.
13

14 **Cell culture.** NCI-H929, HeLa and HCT-116, cells were cultured in RPMI 1640 medium supplemented
15
16 with 10% heat inactivated FBS, 2 mM L-glutamine, 100 U/mL penicillin, 100 µg/mL streptomycin, and
17
18 10 mM HEPES, pH = 7.4 at 37 °C, in 5% CO₂/95% air. Cells were grown at 37 °C in a humidified
19
20 atmosphere with 5% CO₂. All of these cell lines were purchased from the ATCC.
21
22

23 **MTT cell viability assay.** Cell viability was measured using MTT (3-(4,5-dimethylthiazol-2-yl)-2,5-
24
25 diphenyltetrazolium bromide) colorimetric assay. Cells cultured either in 0.1% or 10% serum were
26
27 seeded in 96-well microplates at a density to maintain control (untreated) cells in exponential phase
28
29 of growth during the entire experiment. Cells were incubated with compounds for 48 h followed by
30
31 incubation with 1 mg/mL MTT for 4 h at 37 °C. Lysis buffer (20% SDS) was added and absorbance
32
33 was measured at 540 nm 18 h later. All experiments were repeated at least 2 times in triplicates. The
34
35 percentage of viable cells was calculated and averaged for each well: % growth = (O.D. treated
36
37 cells/O.D. control cells) x 100, and the IC₅₀, concentration reducing by 50% the optical density, was
38
39 calculated by a linear regression performed on the linear zone of the dose-response curve.
40
41
42
43
44
45

46 **Co-immunoprecipitation**

47
48 HeLa cells were transiently transfected, using Effecten reagent (Qiagen), with 3xFlag-tagged BCL-XL
49
50 or MCL-1 expression vectors (p3xFlag-CMV10, Sigma). 24 h later, transfected HeLa cells were treated
51
52 with 18a or 18b during 2 h and harvested in lysis buffer (10 mM HEPES pH 7.5, 150 mM KCl, 5 mM
53
54 MgCl₂, 1 mM EDTA, 0.4% TritonX100), protease and phosphatase inhibitors cocktails (Calbiochem
55
56 539134 and 524625). HeLa cleared lysates were then subjected to immunoprecipitation with anti-
57
58
59
60

1
2
3 Flag M2 agarose beads (Sigma). The immunoprecipitates and inputs were analyzed by immunoblot
4
5 using BAK antibody (BD 556396) or Flag M2 (Sigma).
6
7
8
9
10

11
12 **Mcl-1 stabilisation.** HCT-116 were incubated for 16h with Mcl-1 inhibitors. Total protein extracts of
13
14 HCT-116 cells were generated in lysis buffer (20 mM Tris-HCl, pH 7.4, 135 mM NaCl, 1.5 mM MgCl₂, 1
15
16 mM EDTA, 10% glycerol) containing 1% Triton X-100 and complete protease inhibitors (Roche).
17
18 Protein extracts of the other cell lines were generated in lysis buffer containing 10 mM Hepes pH
19
20 7.4, 142.5 mM KCl, 5 mM MgCl₂, 1 mM EDTA, 1% NP40, protease and phosphatase inhibitors
21
22 cocktails (Calbiochem). Protein content was quantified using the Bradford assay (Bio-Rad). Lysates
23
24 were diluted with LDS sample buffer (Invitrogen) at a 3:1 ratio and denatured at 95 °C for 7-10 min.
25
26 30 µg of protein extracts were separated by SDS:PAGE (NuPAGE 10% Bis Tris gels) and proteins
27
28 transferred onto nitrocellulose membranes. The membranes were blocked in 5% skimmed milk in
29
30 PBS and 0.1% Tween20 (blocking buffer) before incubation with antibodies. Commercially available
31
32 antibodies were used: rabbit polyclonal antibodies against Mcl-1 (Santa Cruz S-19, sc-819), PARP
33
34 (Cell Signaling 9542), and mouse monoclonal antibodies against Actin (Millipore MAB1501R; used as
35
36 a loading control).
37
38
39
40

41 **Immunodetection of cleaved PARP by MesoScale discovery assay.** H929 cells were treated with
42
43 QVD and the indicated compounds in addition to ABT-263 1µM for 6 h and harvested in lysis buffer
44
45 (10 mM Hepes, pH 7.4, 142.5 mM KCl, 5 mM MgCl₂, 1 mM EDTA, 1% NP40, protease and
46
47 phosphatase inhibitors cocktails (Calbiochem). Cleared lysates (5 µg protein) were prepared for
48
49 immunodetection of cleaved PARP or cleaved caspase 3 (markers of apoptosis) by using the MSD
50
51 Apoptosis Panel Whole Cell Lysate kit (MSD) in 96-well plates according to manufacturer's
52
53 instructions, and analysed on the Sector Image 2400.
54
55
56
57
58
59

60 **ASSOCIATED CONTENT**

Supporting Information. Supplementary information with description of chemical synthesis, analysis, co-immunoprecipitation study, structural determination details and the NMR guided model as well Molecular Formula Strings.

Accession Codes. The X-ray structures mentioned in this paper have been deposited in the PDB with the following codes: 6QXJ, 6QYK, 6QZ5, 6QYL, 6QZ6, 6QZ7, 6QZB, 6QZ8, 6QYN, 6QYP, 6QYO.

AUTHOR INFORMATION

Corresponding Author

*Phone: +36 (1) 881-2000. Fax: +36 (1) 881 2011. E-mail: andras.kotschy@servier.com.

ORCID Andras Kotschy: 0000-0002-7675-3864

Present Addresses

†Levente Ondi: XiMo Hungary Ltd., Záhony u. 7., H-1031 Budapest, Hungary

‡Gábor Radics: Hunyadi János u. 34, H-2030 Érd, Hungary

Author contributions

The manuscript was written through contributions of all authors. All authors have given approval to the final version of the manuscript.

ORCID for other authors

ORCID Roderick Hubbard: 0000-0002-8233-7461

ORCID Marton Csekei 0000-0002-5781-1096

ORCID Gabor Radics 0000-0003-4954-3025

ORCID Zoltan B Szabo 0000-0001-7557-0305

ORCID Zoltan Szlavik 0000-0002-9385-806X

■ ACKNOWLEDGMENTS

The authors thank co-workers at the Analytical Division of the Servier Research Institute of Medicinal Chemistry for providing the detailed chemical analysis of the compounds.

■ ABBREVIATIONS USED

Mcl-1, myeloid cell leukemia 1; MCL1, Mcl-1 gene; Bcl-2, B-cell lymphoma 2; Bcl-x_L, B-cell lymphoma extra-large; BH3, Bcl-2 homology domain3; Bim, Bcl-2 like protein 11; FBS, fetal bovine serum; FP, fluorescence polarisation; ITC, isothermal titration calorimetry

References

- ¹ Green, D. R. & Llambi, F. Cell Death Signaling. *CSH Perspect. Biol.* **2015**, *7*, 1-24.
- ² Hanahan, D. & Weinberg, R. A. Hallmarks of cancer: the next generation. *Cell* **2011**, *144*, 646-674.
- ³ Beroukhi, R.; Mermel, C. H.; Porter, D.; Guo Wei, Raychaudhuri, S.; Donovan, J.; Barretina, J.; Boehm, J. S.; Dobson, J.; Urashima, M.; Mc Henry, K. T.; Pinchback, R. M.; Ligon, A. H.; Cho, Y.-J.; Haery, L.; Greulich, H.; Reich, M.; Winckler, W.; Lawrence, M. S.; Weir, B. A.; Tanaka, K. E.; Chiang, D. Y.; Bass, A. J.; Loo, A.; Hoffman, C.; Prensner, J.; Liefeld, T.; Gao, Q.; Yecies, D.; Signoretti, S.; Maher, E.; Kaye, F. J.; Sasaki, H.; Tepper, J. E.; Fletcher, J. A.; Taberero, J.; Baselga, J.; Tsao, M.-S.; Demichelis, F.; Rubin, M. A.; Janne, P. A.; Daly, M. J.; Nucera, C.; Levine, R. L.; Ebert, B. L.; Gabriel, S.; Rustgi, A. K.; Antonescu, C. R.; Ladanyi, M.; Letai, A.; Garraway, L. A.; Loda, M.; Beer, D. G.; True, L. D.; Okamoto, A.; Pomeroy, S. L.; Singer, S.; Golub, T. R.; Lander, E. S.; Getz, G.; Sellers, W. R.; Meyerson, M. The landscape of somatic copy-number alteration across human cancers. *Nature* **2010**, *463*, 899-905.
- ⁴ Akgul, C. Mcl-1 is a potential therapeutic target in multiple types of cancer. *Cell. Mol. Life Sci.* **2009**, *66*, 1326-1336.
- ⁵ Glaser, S. P.; Lee, E. F.; Tronson, E.; Bouillet, P.; Wei, A.; Fairlie, W. D.; Izon, D. J.; Zuber, J.; Rappaport, A. R.; Herold, M. J.; Alexander, W. S.; Lowe, S. W.; Robb, L.; Strasser, A. Anti-apoptotic Mcl-1 is essential for the development and sustained growth of acute myeloid leukemia. *Gene. Dev.* **2012**, *26*, 120-125.
- ⁶ Kelly, G. L.; Grabow, S.; Glaser, S. P.; Fitzsimmons, L.; Aubrey, B. J.; Okamoto, T.; Valente, L. J.; Robati, M.; Tai, L.; Fairlie, W. D.; Lee, E. F.; Lindstrom, M. S.; Wiman, K. G.; Huang, D. C. S.; Bouillet, P.; Rowe, M.; Rickinson, A. B.; Herold, M. J.; Strasser, A. Targeting of MCL-1 kills MYC-driven mouse and human lymphomas even when they bear mutations in p53. *Gene. Dev.* **2014**, *28*, 58-70.

⁷ Koss, B.; Morrison, J.; Perciavalle, R. M.; Singh, H.; Rehg, J. E.; Williams, R. T.; Opferman, J. T. Requirement for antiapoptotic MCL-1 in the survival of BCR-ABL B-lineage acute lymphoblastic leukemia. *Blood* **2013**, *122*, 1587-1598.

⁸ a) Song, L.; Coppola, D.; Livingston, S.; Cress, D.; Haura, E. B. Mcl-1 regulates survival and sensitivity to diverse apoptotic stimuli in human non-small cell lung cancer cells. *Cancer Biol. Ther.* **2005**, *4*, 267-276. b) Zhang, H.; Guttikonda, S.; Roberts, L.; Uziel, T.; Semizarov, D.; Elmore, S. W.; Levenson, J. D.; Lam, L. T. Mcl-1 is critical for survival in a subgroup of non-small-cell lung cancer cell lines. *Oncogene* **2011**, *30*, 1963-1968.

⁹ a) Wei, G.; Margolin, A. A.; Haery, L.; Brown, E.; Cucolo, L.; Julian, B.; Shehata, S.; Kung, A. L.; Beroukhim, R.; Golub, T. R. Chemical genomics identifies small-molecule MCL1 repressors and BCL-xL as a predictor of MCL1 dependency. *Cancer Cell* **2012**, *21*, 547-562. b) Barlaam, B.; De Savi, C.; Drew, L.; Ferguson, A.; Ferguson, D.; Gu, C.; Hawkins, J. W.; Hird, A.; Lamb, M.; O'Connell, N.; Pike, K.; Proia, T.; San Martin, M.; Vasbinder, M.; Varnes, J.; Wang, J.; Shao, W. Discovery of AZD4573, a potent and selective inhibitor of CDK9 that enables transient target engagement for the treatment of hematologic malignancies. *Cancer Res.* **2018**, *78*, 1650-1650.

¹⁰ Juin, P., Geneste, O., Gautier, F., Depil, S. & Campone, M. Decoding and unlocking the BCL-2 dependency of cancer cells. *Nat. Rev. Cancer* **2013**, *13*, 455-465.

¹¹ a) Levenson, J. D.; Zhang, H.; Chen, J.; Tahir, S. K.; Phillips, D. C.; Xue, J.; Nimmer, P.; Jin, S.; Smith, M.; Xiao, Y.; Kovar, P.; Tanaka, A.; Bruncko, M.; Sheppard, G. S.; Wang, L.; Gierke, S.; Kategaya, L.; Anderson, D. J.; Wong, C.; Eastham-Anderson, J.; Ludlam, M. J. C.; Sampath, D.; Fairbrother, W. J.; Wertz, I.; Rosenberg, S. H.; Tse, C.; Elmore, S. W.; Souers, A. J. Potent and selective small-molecule MCL-1 inhibitors demonstrate on-target cancer cell killing activity as single agents and in combination with ABT-263 (navitoclax). *Cell Death Dis.* **2015**, *6*, e1590. b) Pelz, N. F.; Bian, Z.; Zhao, B.; Shaw, S.; Tarr, J. C.; Belmar, J.; Gregg, C.; Camper, D. M.; Goodwin, C. M.; Arnold, A. L.; Sensintaffar, J. L.; Friberg, A.; Rossanese, O. W.; Lee, T.; Olejniczak, E. T.; Fesik, S. W. Discovery of 2-Indole-acylsulfonamide Myeloid Cell Leukemia 1 (Mcl-1) Inhibitors Using Fragment-Based Methods. *J. Med. Chem.* **2016**, *59*, 2054-2066.

¹² a) Kotschy, A.; Szlavik, Z.; Murray, J.; Davidson, J.; Maragno, A. L.; Le Toumelin-Braizat, G.; Chanrion, M.; Kelly, G. L.; Gong, J.; Moujalled, D. M.; Bruno, A.; Csekei, M.; Paczal, A.; Szable, Z. B.; Sipos, S.; Radics, G.; Prosenyak, A.; Balint, B.; Ondi, L.; Blasko, G.; Robertson, A.; Surgenor, A.; Dokurno, P.; Chen, I.; Matassova, N.;

1
2
3
4
5
6
7
8
9
10
11
12
13
14
15
16
17
18
19
20
21
22
23
24
25
26
27
28
29
30
31
32
33
34
35
36
37
38
39
40
41
42
43
44
45
46
47
48
49
50
51
52
53
54
55
56
57
58
59
60

Smith, J.; Pedder, C.; Graham, C.; Studeny, A.; Lysiak-Auvity, G.; Girard, A.; Gravé, F.; Segal, D.; Riffkin, C. D.; Pomilio, G.; Galbraith, L. C. A.; Aubrey, B. J.; Brennan, M. S.; Herold, M. J.; Chang, C.; Guasconi, G.; Cauquil, N.; Melchiorre, F.; Guigal-Stephan, N.; Lockhart, B.; Colland, F.; Hickman, J. A.; Roberts, A. W.; Huang, D. C. S.; Wei, A. H.; Strasser, A.; Lessene, G.; Geneste, O. The MCL1 inhibitor S63845 is tolerable and effective in diverse cancer models. *Nature* **2016**, *538*, 477–482. b) Caenepeel, S.; Brown, S. P.; Belmontes, B.; Moody, G.; Keegan, K. S.; Chui, D.; Whittington, D. A.; Huang, X.; Poppe, L.; Cheng, A. C.; Cardozo, M.; Houze, J.; Li, Y.; Lucas, B.; Paras, N. A.; Wang, X.; Taygerly, J. P.; Vimolratana, M.; Zancanella, M.; Zhu, L.; Cajulis, E.; Osgood, T.; Sun, J.; Damon, L.; Egan, R. K.; Greninger, P.; McClanaghan, J. D.; Gong, J.; Moujalled, D.; Pomilio, G.; Beltran, P.; Benes, C. H.; Roberts, A. W.; Huang, D. C.; Wei, A.; Canon, J.; Coxon, A.; Hughes, P. E. AMG 176, a selective MCL1 Inhibitor, is effective in hematological cancer models alone and in combination with established therapies. *Cancer Discov.* **2018**, *8*, 1582-1597. c) Johannes, J. W.; Bates, S.; Beigie, C.; Belmonte, M. A.; Breen, J.; Cao, S.; Centrella, P. A.; Clark, M. A.; Cuzzo, J. W.; Dumelin, C. E.; Ferguson, A. D.; Habeshian, S.; Hargreaves, D.; Joubran, C.; Kazmirski, S.; Keefe, A. D.; Lamb, M. L.; Lan, H.; Li, Y.; Ma, H.; Mlynarski, S.; Packer, M. J.; Rawlins, P. B.; Robbins, D. W.; Shen, H.; Sigel, E. A.; Soutter, H. H.; Su, N.; Troast, D. M.; Wang, H.; Wickson, K. F.; Wu, C.; Zhang, Y.; Zhao, Q.; Zheng, X.; Hird, A. W. Structure based design of non-natural peptidic macrocyclic Mcl-1 inhibitors. *ACS Med. Chem. Lett.* **2017**, *8*, 239–244. d) Shaw, S.; Bian, Z.; Zhao, B.; Tarr, J. C.; Veerasamy, N.; Ok, K.; Johannes Belmar, L.; Arnold, A. L.; Fogarty, S. A.; Perry, E.; Sensintaffar, J. L.; Camper, D. V.; Rossanese, O. W.; Lee, T.; Olejniczak, E. T.; Fesik, S. W. Optimization of potent and selective tricyclic indole diazepinone Myeloid Cell Leukemia-1 inhibitors using structure-based design. *J. Med. Chem.* **2018**, *61*, 2410–2421. e) Bruncko, M.; Wang, L.; Sheppard, G. S.; Phillips, D. C.; Tahir, S. K.; Xue, J.; Erickson, S.; Fidanze, S.; Fry, E.; Hasvold, L.; Jenkins, G. J.; Jin, S.; Judge, R. A.; Kovar, P. J.; Madar, D.; Nimmer, P.; Park, C.; Petros, A. M.; Rosenberg, S. H.; Smith, M. L.; Song, X.; Sun, C.; Tao, Z-F.; Wang, X.; Xiao, Y.; Zhang, H.; Tse, C.; Levenson, J. D.; Elmore, S. W.; Souers, A. J. Structure-guided design of a series of MCL-1 inhibitors with high affinity and selectivity. *J. Med. Chem.* **2015**, *58*, 2180–2194.

¹³ Murray, J.; Davidson, J.; Chen, I.; Dokurno, P.; Davis, B.; Harris, R.; Jordan, A.; Matassova, N.; Pedder, C.; Ray, S.; Roughley, S.; Smith, J.; Walmsley, C.; Wang, Y.; Whitehead, N.; Williamson, D.; Casara, P.; Le Diguarher, T.;

1
2
3
4 Hickman, J.; Stark, J.; Kotschy, A.; Geneste, O.; Hubbard, R.E. Establishing drug discovery and identification of
5 hit series for the anti-apoptotic proteins, Bcl-2 and Mcl-1; *ACS Omega* **2019**, *4*, 8892-8906.

6
7
8 ¹⁴ All computational work was done using Schrodinger software, except for the protein conformation
9 ensemble which was prepared by MOE from Chemical Computing Group.

10
11
12 ¹⁵ DeGoey, D.A.; Chen, H-J.; Cox, P.B.; Wendt, M.D. Beyond the rule of 5: lessons learned from AbbVie's drugs
13 and compound collection. *J. Med. Chem.* **2018**, *61*, 2636-2651.
14
15
16
17
18
19
20
21
22
23
24
25
26
27
28
29
30
31
32
33
34
35
36
37
38
39
40
41
42
43
44
45
46
47
48
49
50
51
52
53
54
55
56
57
58
59
60

TOC GRAPHIC

